Electronic Supplementary Material (ESI) for Journal of Materials Chemistry B.

Supplementary Information

A tumor-targeted, intracellular activatable and theranostic nanodiamond drug platform for in vivo strongly enhanced antitumor therapy

Xiangbin Du,[a#] Lin Li,[b,c#] Shiguo Wei,[a] Songbai Wang,[a] Yingqi Li[a,b*]

[a]Department of Chemistry, College of Chemistry and Chemical Engineering, Shanxi University, Taiyuan 030006, PR China

[b]Key Laboratory of Chemical Biology and Molecular Engineering of Ministry of Education, Institute of Molecular Science, Shanxi University, Taiyuan 030006, PR China

[c]Department of Chemistry, Taiyuan Normal University, Jinzhong 030619, PR China.

030619, PR China.

***Corresponding Authors:**

Telephone: +86-351-7010588

E-mail: wkyqli@sxu.edu.cn

Dynamic light scattering (DLS) analysis was performed to measure the particle size and zeta potential (Table S1). Compared with pristine ND, the average size of the nanoparticles by layer-by-layer synthesis was increased, and the zeta potentials changed accordingly, which is indicative of surface binding. The NPHF/D had a larger particle size of 264.1 ± 0.8 nm with a PDI of 0.058, which could greatly benefit their aggregation in the tumor site because of the well-known enhanced permeability and retention (EPR) effect in which tumor blood vessels can retain 100-400 nm particles. Besides, after the layers of modification, the PDI of the nanoparticles is gradually reduced, indicating the dispersity of the nanoparticles was improved accordingly.

Table S1 Particle size, zeta potential and PDI for various nanoparticles

Nanoparticle	Size（nm）	Zeta potential（mV）	PDI
ND	**166.0±1.6**	**-30.2±1.0**	**0.164**
NP	**184.6±6.4**	**-24.7±1.9**	**0.126**
NPH	**194.8±2.8**	**0.04±0.2**	**0.111**
NPHF	**210.1±2.1**	**0.02±0.1**	**0.096**
NPHF/D	**264.1±0.8**	**-19.7±0.6**	**0.058**

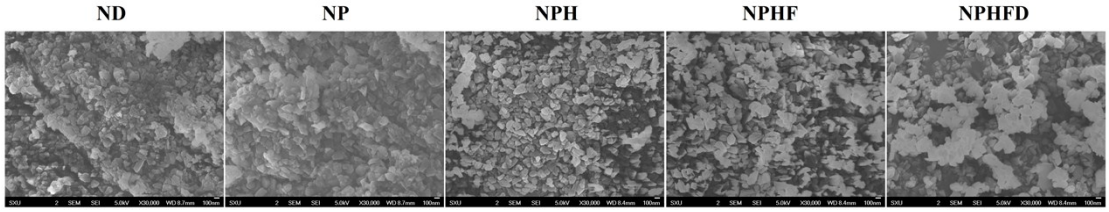

Fig. S1 Typical SEM images before and after coating with different molecules, respectively. The scale bars represent 100 nm.

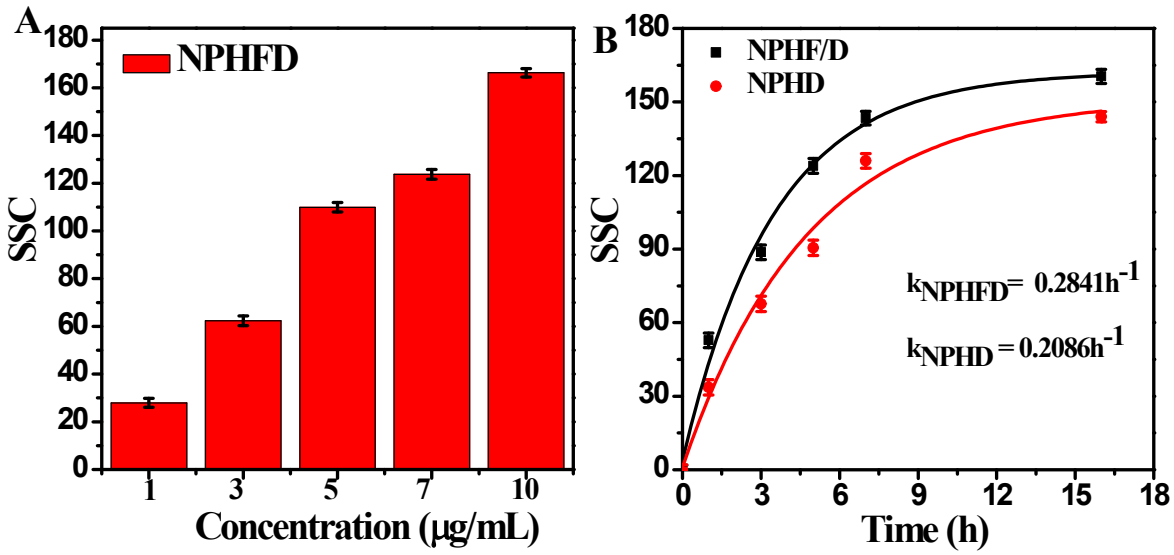

Fig. S2 Effect of interacting concentration and time on intake of NPHF/D by HepG2 cells. (A) Effect of incubating concentration on intake of NPHF/D by HepG2. (B) Effect of interacting time on intake of NPHD and NPHF/D by HepG2.

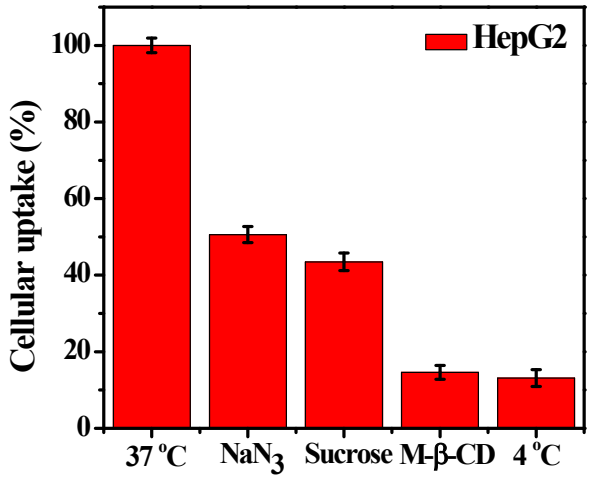

Fig. S3 Quantitative analysis of mechanistic study of the uptake of NPHF under different treatment conditions.

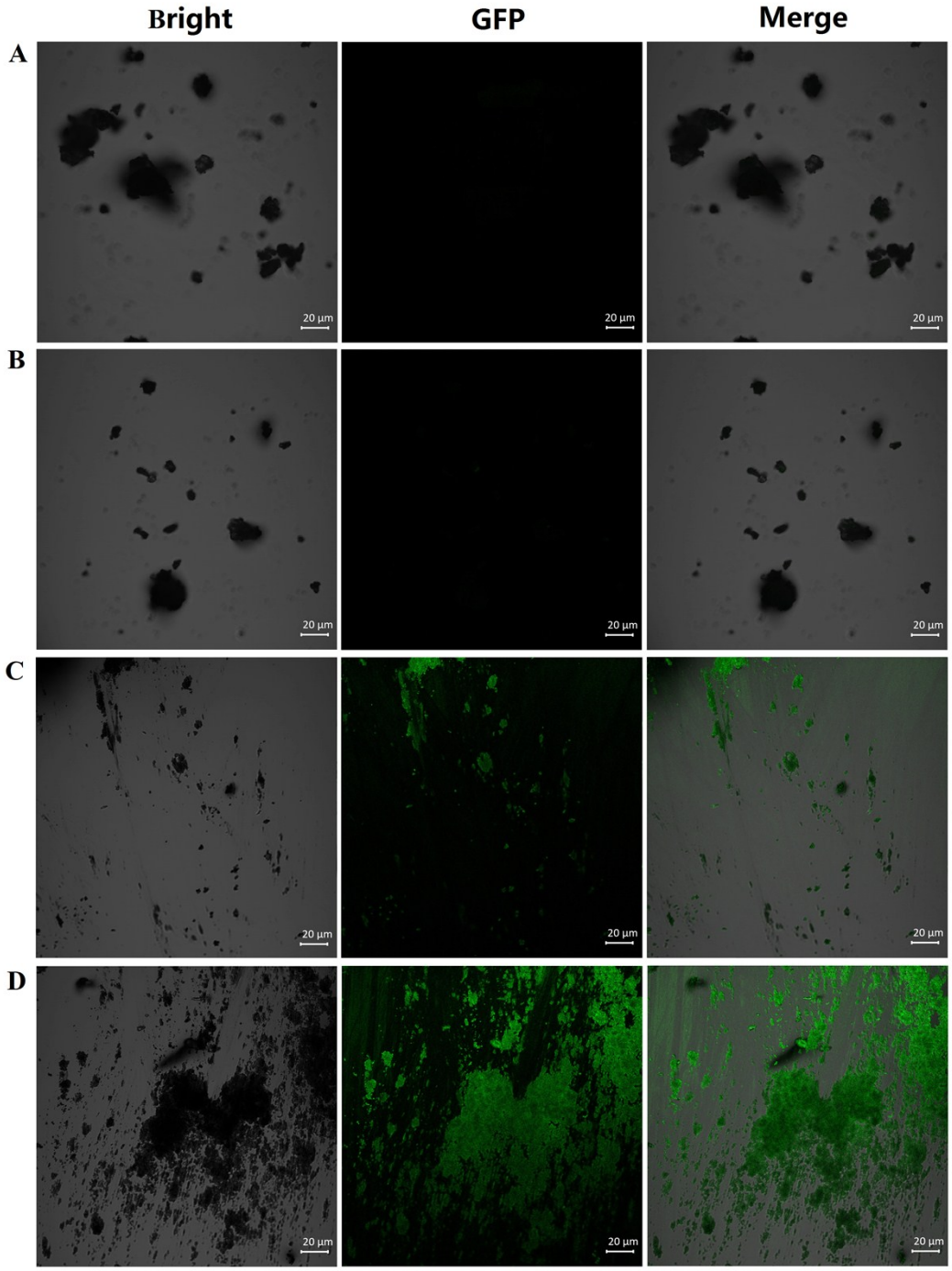

Fig. S4 Brightfield and green fluorescence images of different nanoparticles attached to glass coverslip. (A) carboxylated ND; (B) NPHF/D; (C) NPD (ND-PEG nanoparticles physical adsorption DOX, which is prepared according to our previous method.[1]); (D) free DOX via laser confocal microscope with excitation wavelengths of 488 nm and the fluorescence was collected from 500 to 545 nm.

In order to confirm the intracellular localization of NPHF/D or NPHD, we used the staining co-localization method with laser scanning confocal microscope (LSCM),

where the green fluorescent signal was from DOX detached from NPHF/D or NPHD and the red fluorescent was from lysosomes marked with fluorescent dyes. After chasing their endocytosis for 5 h, the red fluorescent and the green fluorescence was observed in Fig. S5. Some orange fluorescence in the cytoplasm was observed, which showed the high colocalization of nanoparticles with lysosomes marked in red, and the colocalization coefficient (Manders' correlation coefficient) is 0.74 and 0.72 in the Fig. S5. Generally, when a colocalization coefficient is approximate to or greater than 0.5 ($r \geqslant 0.5$), it can be considered as indicator of good colocalization. So it can be thought that NPHF/D or NPHD particles can be trapped inside the lysosomes.

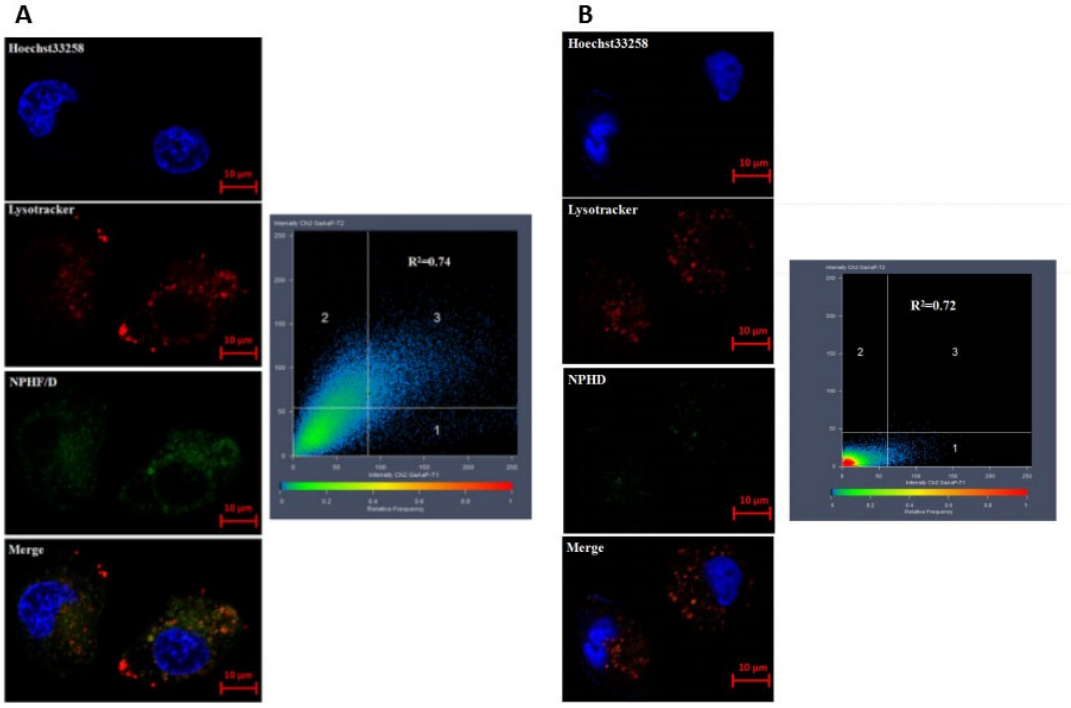

Fig. S5 Intracellular accumulation of NPHF/D (A) and NPHD (B) bioconjugates after endocytosis in HepG2 cells after 5 h, respectively. The upper images in the left column show the cell nucleus dyed with H33258; the second images in the left column shows red fluorescence for lysosomes labeling by lyso-tracker probe; the third images in the left column shows green fluorescence from the DOX; the bottom images in the left column shows the merged fluorescence image of lysosomes and NPHF/D or NPHD; the right images represents the scatter plot of colocalization (r = 0.74, 0.72, respectively).

We further compared the cytotoxicity of NPHD and NPHF/D nanoparticles by apoptosis analysis. As shown in Fig. S6A, NPH (b) and NPHF (c) had hardly induced cell apoptosis similar to blank control (a), which verified its excellent biocompatibility and is also highly consistent with the MTT assay. On the contrary, after 24 h incubation, NPHF/D (e) induced 96% of HepG2 cells apoptosis, far more efficient than NPHD (d, 26%) and DOX (e, 29%) as that found by MTT assay. The MTT assay and apoptosis analysis data suggested that NPHF/D nanoparticles efficiently delivered DOX into HepG2 cells via FA-enhanced internalization, where DOX was reactivated by pH-mediated.

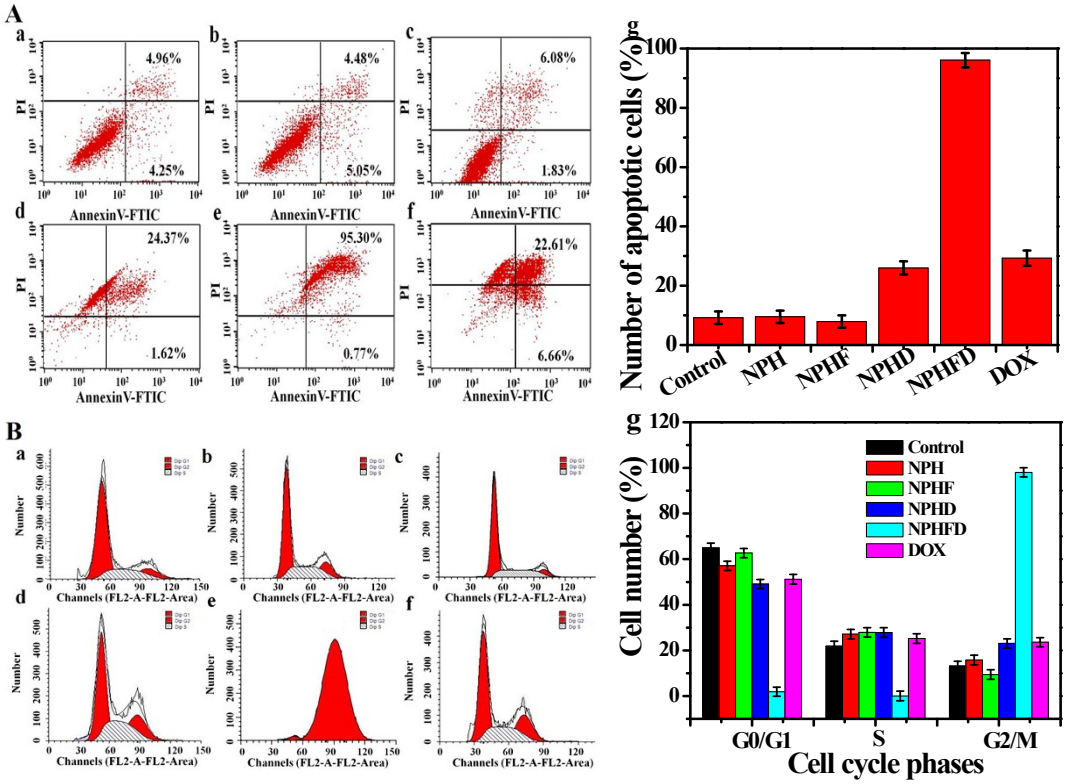

Fig. S6 Apoptosis and cell cycle detection determined by various nanomaterials using flow cytometry analysis. (A) Apoptosis of HepG2 cells induced by NPH (b), NPHF (c), NPHD (d), NPHF/D (e), and DOX (f) for 24 h, respectively, HepG2 cells untreated as control (a), the number of apoptotic cells (g), where data were adopted from a-f. (B) Cell cycle of HepG2 cells induced by NPH (b), NPHF (c), NPHD (d), NPHF/D (e), and DOX (f) for 12 h, HepG2 cells untreated as control (a), the cell cycle histogram (g), where data were adopted from a-f.

The cell cycle distributions of HepG2 cells were also determined by flow cytometry. As shown in Fig. S6B, the cells treated with NPH (b) and NPHF (c) exhibited similar cell cycle with control cells (a), while NPHD (d), NPHF/D (e) and free DOX (f) significantly changed the cell cycle, resulting in 9.91%, 84.93% and 10.5% increase in the percentage of G2/M phase, respectively, which implied that NPHD, NPHF/D and free DOX can change the cell cycle and mainly block in G2/M phase.

References:

1. L. Li, L. Tian, Y. Wang, W. Zhao, F. Cheng, Y. Li, B. Yang, J. Mater. Chem. B, 2016, 4, 45046-45058.